

Research on Online Measurement Method for Small Workpiece Circular Holes Based on Machine Vision

Yan-Chao Sun^{1,2}, Liang-Gui Zhang^{1*}, Wen-Tao Li¹

¹ Department of mechanical engineering, Hebei Institute of Mechanical and Electrical Technology,
Xingtai City 054000, Hebei Province, China
{yanchao0986, lianggui3897, wentao3982}@163.com

² Xingtai Metal Processing Equipment Intelligent Integration and Diagnosis Technology Innovation Center,
Xingtai City 054000, Hebei Province, China

Received 27 March 2024; Revised 2 April 2024; Accepted 15 April 2024

Abstract. In modern manufacturing, due to the narrow format, short size, and complex surface structure of small-sized workpieces, automatic detection of surface defects, dimensions, etc. on small-sized workpieces faces difficulties, making it difficult to meet the requirements of fully automated production lines. Especially, there is no good solution to the problem of high-precision automatic measurement of geometric features of circles and arcs on small-sized workpieces. This article takes the engine end cover circular hole thermal component as the research object, builds a hardware platform for image acquisition of small-sized workpieces based on machine vision, proposes an online size measurement method for small-sized circular holes, and realizes the measurement of the position size and aperture size of small-sized product shell workpieces. In order to achieve the above methods, this article builds a visual detection hardware system and describes a detailed machine vision hardware selection scheme. Then, the images collected by the system are preprocessed, including image denoising, image correction, and image feature extraction. Then, for the processed images, an improved Hough transform fitting method is used to obtain the online size of features. In order to visualize the results, the detection system and software are designed according to the actual application scenario. The overall scheme of this article is efficient and reasonable, and the detection result error is within a reasonable range.

Keywords: visual measurement, small size workpieces, online detection

1 Introduction

Intelligent manufacturing technology is the core force driving China's manufacturing industry from a manufacturing powerhouse to a manufacturing powerhouse. In modern manufacturing, mechanical equipment, electronic products, tool parts, etc. are becoming increasingly precise and complex. Precise and complex equipment is generally composed of small-sized workpieces, which need to undergo quality monitoring after production and processing [1]. Dimensional error detection is the most important part of part quality inspection, generally including position dimension detection and shape dimension detection.

However, currently in the quality inspection process, based on existing size inspection methods and equipment, there are still the following difficulties that need to be solved in the workpiece quality inspection process:

1) Small size workpieces often have complex structural features and diverse processing methods, resulting in a tight surface structure. It is necessary to identify the target object in the tight structural features, which can lead to recognition errors. In addition, due to the small size of the structure, even small measurement errors can lead to significant accuracy deviations [2].

2) From the perspective of measurement methods, when measuring small-sized parts, the detection method mainly relies on direct observation with the naked eye or using contact mechanical tools such as gauges, calipers, and micrometers for step-by-step detection. This method has low measurement efficiency and accuracy, and poor detection repeatability.

3) Some quality inspection processes use visual inspection, while conventional visual inspection is static. The measured object remains stationary and the position does not change. At the same time, in the past, visual inspection was mostly offline. During offline inspection, the part leaves the production station, causing changes

* Corresponding Author

in the inspection coordinate system, increasing the generation of measurement errors, and resulting in inaccurate measurement results. At the same time, during the repeated clamping process of the part, positioning errors will be generated, which will actually affect the machining accuracy of the part [3].

In response to the above situation, the development of dynamic machine vision technology provides an effective solution to solve the technical difficulties in quality inspection. In response to the above problems, this article uses machine vision technology to measure small-sized workpieces. Finally, taking the measurement of the engine end cover installation hole as an example, the feasibility of the method is verified. The work done in the article is as follows:

1) We have built a visual inspection system and provided a detailed description of the parameters and models of each hardware device in the system.

2) In order to improve the accuracy of visual detection, visual graphics are preprocessed, which includes image correction, image denoising, and image feature extraction.

3) Design and implementation of an online measurement scheme for image features, and completion of the development of an image measurement system.

In order to clearly describe the work done in this article, the structure of the article is arranged as follows: Chapter 2 mainly introduces the research work related to this article, Chapter 3 mainly describes the construction of the visual system, Chapter 4 describes the image processing process, Chapter 5 describes the methods of online measurement, Chapter 6 completes the design of the measurement system, and Chapter 7 is the conclusion.

2 Related Works

Many domestic scholars have conducted research on machine vision measurement technology. Haojing Bao, based on the shape characteristics of the sprocket tooth profile, used the highest point array and the lowest point array to obtain the contour diameter through elliptical fitting. Combined with the external parameter calibration method based on quadratic curve invariance, the diameter measurement error of the sprocket tooth root circle and tooth top circle is less than 40% μm [4].

Chao Bi, the research object is unconventional leaf shaped holes. A visual system was built, and multiple local images of the leaf shaped holes were collected, then concatenated to obtain their panoramic images. Finally, the geometric dimensions and contour parameters of the measured leaf shaped holes were obtained through image processing and leaf shape parameter analysis [5].

Xuang Chen mainly studied dynamic measurement, measuring circular holes. The dynamically collected circular hole images were preprocessed, and edge detection and gradient methods were used to obtain the center and radius of the outer circle. Combined with iterative fitting methods, dynamic measurement of the dimensions on both sides of the circular hole was achieved. Finally, under a certain lighting condition, the measurement error was less than 1 pixel [6].

Zichao Shu uses a 3D camera to capture product dimensions from a top-down angle. With the assistance of product 3D information, precise 2D image segmentation and corner 2D coordinate positioning are achieved. Then, the 3D coordinates are obtained by converting the 2D coordinates and depth information, and the product size is calculated [7].

Shijing Zhang from Anhui University of Technology proposed a machine vision measurement system for internal thread pitch parameters based on the principle of spherical reflection panoramic imaging, which achieved non-contact measurement of internal threads. The system was compared with the pitch measurement values of conventional thread measurement machines, and the experimental results showed that the average measurement error of the system was 0.0185 mm, meeting the requirements of internal thread pitch accuracy in industrial production and improving detection efficiency [8].

Shuaikang Li, in order to achieve high-precision non-contact measurement of gear end face height, proposed a gear end face height measurement method based on binocular stereo vision. The image was obtained using a monocular CCD camera with a sliding fixed baseline distance. After correction, the SGBM algorithm was used to perform stereo matching on the corrected binocular image. The experimental results showed that the proposed measurement system and method have high accuracy and stability [9].

The non-contact measurement method is not only efficient, but also continuously improves the measurement progress. The visual system, image processing, and measurement algorithms are the three stages of completing visual online measurement. However, there is still room for improvement in measurement methods and accuracy.

Therefore, after analyzing the research results of various scholars, the research direction and methods of this article are determined.

3 Construction of Visual Inspection System

The visual inspection system mainly includes four main parts: camera, lens, light source, and computer. The main electronic component of a camera is an image sensor, which is used to convert photoelectric signals and achieve A/D conversion, ultimately transmitting them to a computer to form an image, equivalent to the retina of the human eye [10]. The function of a lens is to concentrate light on the imaging plane, and its principle is similar to the lens of the human eye. The selection of cameras is mainly determined by the size and accuracy requirements of the object being measured. The size of the object being measured determines the field of view, which represents the actual size range of the scene received by the image sensor. Lighting is the most important factor affecting image quality, which determines the complexity of processing algorithms and directly affects detection efficiency and accuracy. In summary, the equipment and parameter names selected in this article are shown in Table 1. The system structure is shown in Fig. 1.

Table 1. System equipment name and parameters

	Parameter name	Parameter values
Camera	Model	mV-GEC2000
	Resolving power	3672*5488
	Target surface size	1/3°
	Full resolution	40 fps
	Pixel size	3.75 μm ×3.75 μm
	Signal-to-noise ratio	46dB
Lens	Resolving power	5M
	Focal length	16
	Image size	1/1.8°
	External dimensions	29.3*25.1
	Field of view angle	18.2°
	Distortion	<0.06%
Light source	Interface	c
	Light source type	LED
	Light source controller	aFT-ALP2409-02

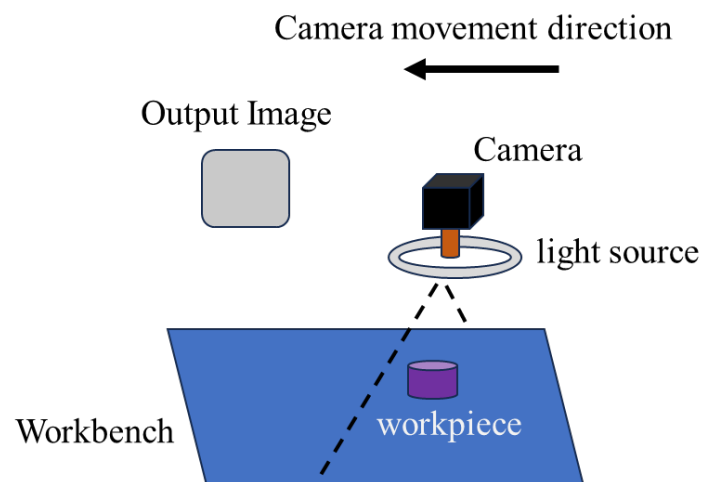


Fig. 1. Image acquisition system model

The selection of visual system requires full consideration of the detection environment, including the selection of light sources, cameras, lenses, image sensors, acquisition cards, interfaces, etc. In the application scenario of this article, the maximum diameter of the target detection object is 114.72 millimeters, and the diameter of the mounting hole on it is 3.21 millimeters. To ensure that the target detection object can be fully presented in the image, the horizontal field of view of the camera should be greater than the maximum horizontal size of the target detection object. Therefore, the horizontal field of view of the camera is designed to be 150mm [11].

$$P_{value} = \frac{F_x}{p_a}. \quad (1)$$

$$M_a = \frac{l_{sensor}}{F_x}. \quad (2)$$

$$F_a = M_a * L_w. \quad (3)$$

P_{value} - Camera unidirectional pixels;
 F_x - Unidirectional field of view;
 p_a - Target detection accuracy;
 M_a - Magnification rate;
 l_{sensor} - Sensor size;
 F_a - Focal length;
 L_w - Working distance.

The images collected in industrial scenes are often mixed with environmental interference factors, so the target detection accuracy in pixel estimation needs to be 5 times the required indicators, that is, the target detection accuracy needs to be 0.02mm. According to equation (1), the horizontal pixels of the array camera should be at least 3000. At the same time, considering the accuracy loss during image processing, the theoretical accuracy requirement of industrial cameras is higher than the target detection accuracy. Therefore, the linear array camera selected in this article is 3672 * 5488 pixels.

Given the parameters such as pixel size, resolution, field of view, and estimated working distance of the camera, the estimated focal length $f = 106\text{mm}$ can be used to determine that there are 116mm lenses adjacent to the focal length threshold.

When the visual system is working, in order to ensure that the workpiece is within the camera imaging range and the image is obtained smoothly, it is necessary to fix the visual system on the assembly line and install it with fixtures; After fixing it, initialize the system and set the stroke, speed, and other parameters of the motion module based on the movement speed of the detection Engine end cover, as well as the control parameters of the visual system such as line frequency, line period, and exposure time, to ensure that the Engine end cover is fully captured and the image is not stretched or compressed. At this point, the workpiece is clearly imaged in the middle position of the image. The control system sends a signal to the visual system to start collecting the image. After the visual system completes the data acquisition process, the collected data is transmitted to the computer terminal for processing. By performing image calculation on the Engine end cover end face image, the position size, diameter, roundness, and other information of the Engine end cover installation hole are analyzed and calculated based on the contour characteristics of the workpiece. Finally, a report is generated in the PC testing system and the results are displayed.

In summary, after determining the hardware selection of the visual system, the overall scheme for online detection system detection is shown in Fig. 2.

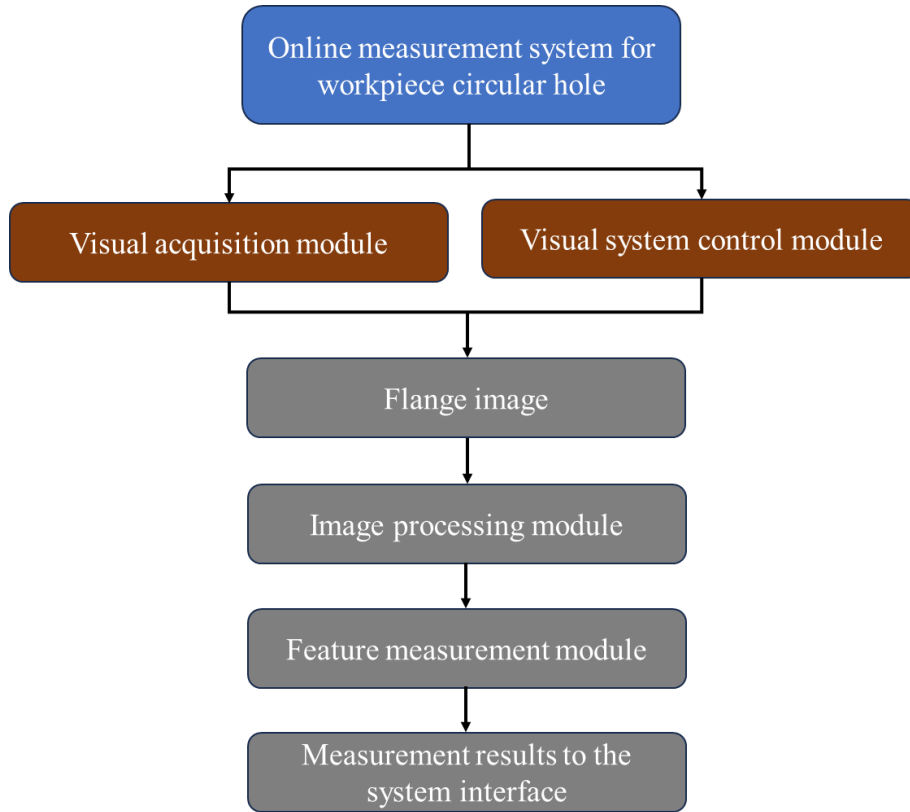


Fig. 2. Overall scheme of detection system

4 Preprocessing of Workpiece Images

In the image processing stage, the camera needs to be calibrated first. During the visual measurement process, the camera maps three-dimensional spatial information to two-dimensional images. In order to determine the transformation relationship between spatial points and pixel coordinates, it is necessary to establish a camera imaging model and calculate the transformation matrix parameters [12]. In this paper, Zhengyou Zhang calibration method is used to calibrate the black and white chessboard with a chessboard grid of 12*9.

Firstly, the camera coordinate system undergoes rotation and translation relative to the world coordinate system, which can be transformed using a pose matrix. The representation method is as follows:

$$\begin{bmatrix} X_c \\ Y_c \\ Z_c \\ 1 \end{bmatrix} = \begin{bmatrix} R_{3*3} & T_{3*1} \\ 0 & 1 \end{bmatrix} \begin{bmatrix} X_w \\ Y_w \\ Z_w \\ 1 \end{bmatrix} = [r_1 \quad r_2 \quad t] \begin{bmatrix} X_w \\ Y_w \\ Z_w \\ 1 \end{bmatrix}. \quad (4)$$

In the formula, $[r_1 \quad r_2 \quad t]$ represents the extrinsic matrix. For ease of calculation, it is assumed that the calibration board is located in the $X_w O_w Y_w$ plane. Secondly, based on the principle of projection perspective, convert the camera coordinate system to the image coordinate system. Assuming there is a point in the camera coordinate system, without considering image distortion, the coordinates of imaging point $P(x_p, y_p)$ in the image coordinate system are:

$$z_c \begin{bmatrix} x_p \\ y_p \\ 1 \end{bmatrix} = \begin{bmatrix} F_a & \gamma & 0 \\ 0 & F_a & 0 \\ 0 & 0 & 1 \end{bmatrix} \begin{bmatrix} x_c \\ y_c \\ z_c \end{bmatrix}. \quad (5)$$

γ is the image distortion coefficient, and the conversion relationship from the world coordinate system to the pixel coordinate system is:

$$\begin{bmatrix} u \\ v \\ 1 \end{bmatrix} = \frac{1}{z_c} \begin{bmatrix} a & \gamma & u_0 \\ 0 & \beta & v_0 \\ 0 & 0 & 1 \end{bmatrix} \begin{bmatrix} r_1 & r_2 & t \end{bmatrix} \begin{bmatrix} x_W \\ y_W \\ 1 \end{bmatrix}. \quad (6)$$

(u, v) -Pixel coordinates can be obtained from the image;

(x_W, y_W) -Checkerboard corner coordinates in the world coordinate system.

Introduce the hard matrix H , whose expression is:

$$\begin{aligned} H &= \frac{1}{z_c} \begin{bmatrix} a & \gamma & u_0 \\ 0 & \beta & v_0 \\ 0 & 0 & 1 \end{bmatrix} \begin{bmatrix} r_1 & r_2 & t \end{bmatrix} \\ &= sA \begin{bmatrix} r_1 & r_2 & t \end{bmatrix}. \end{aligned} \quad (7)$$

s - Scale factor.

After the above process, camera calibration is completed. After camera calibration, the camera preprocesses the collected images to enhance the features of the recognized object, reduce interference, and improve measurement accuracy. The preprocessing of workpiece images includes correcting the images captured by the camera, denoising the images, and feature extraction for circular hole features.

4.1 Image Correction

In the production process, the camera needs to continuously capture the Engine end cover end cover, and the presence of vibration, signal disturbance, and other situations in the production line can cause distortion in the visual image obtained. Therefore, it is necessary to correct the image. The purpose of correction is to achieve alignment between RGB images and depth images. Camera correction is achieved through the Zhengyou Zhang calibration method [13]. For a calibrated camera, its internal and external parameter matrices, as well as distortion parameters, are known. Due to the presence of nonlinear geometric distortion in the camera, there is geometric distortion between the target point and the theoretical image point. Therefore, it is necessary to correct the radial and tangential distortions of the camera. The mathematical model expressions for radial and tangential distortions are:

$$\begin{cases} x_{rad} = x_o \left(1 + \lambda_1 r^2 + \lambda_2 r^4 + \lambda_3 r^6 \right) \\ y_{rad} = y_o \left(1 + \lambda_1 r^2 + \lambda_2 r^4 + \lambda_3 r^6 \right) \end{cases}. \quad (8)$$

$$\begin{cases} x_{tan} = x_o + 2\delta_1 x_o y_o + \delta_2 \left(r^2 + 2x_o^2 \right) \\ y_{tan} = y_o + 2\delta_1 x_o y_o + \delta_2 \left(r^2 + 2x_o^2 \right) \end{cases}. \quad (9)$$

In the formula, (x_o, y_o) is the position coordinate of the normal image, (x_{rad}, y_{rad}) is the position coordinate of the distorted image, r is the distance from the center of the imaging device, and $\lambda_{i(i=1, 2, 3)}$ is the radial distortion coefficient. $\delta_{j(j=1, 2)}$ is the radial distortion coefficient. By using physical dimensions and pixel scale factors, distorted image coordinates can be obtained, and then pixel values can be interpolated to obtain distorted images.

When the intrinsic and extrinsic matrix of the camera is known, alignment between RGB images and depth images can be achieved through matrix transformation, and the coordinate transformation relationship is represented as follows:

$$d_c \begin{bmatrix} u \\ v \\ 1 \end{bmatrix} = A_1 A_2 \begin{bmatrix} x_a \\ y_a \\ z_a \\ 1 \end{bmatrix}. \quad (10)$$

In the formula, d_c is the depth value of point (u, v) in the non distorted image, A_1 is the camera intrinsic matrix, A_2 is the camera extrinsic matrix, and (x_a, y_a, z_a) is the world coordinate of the point. After the above transformation, it is possible to map two-dimensional points in the depth map to RGB images, achieving image alignment.

Set the bottom left corner of the digital image as the first input point, while ensuring that the coordinates of other input points remain unchanged. The specific expression is:

$$(x_{01}, y_{01}) = (x_n, y_n). \quad (11)$$

If the input point in the bottom right corner of the digital image is used as the second input point, the corresponding output point row coordinates will be the same as the first output point row coordinates:

$$(x_{02}, y_{02}) = (x_{01} + d, y_{01} + d). \quad (12)$$

d represents the distance between input points, with the input point in the upper left corner as the third input point, and η represents the aspect ratio. The specific calculation formula is:

$$(x_{03}, y_{03}) = (x_{01} - d \cdot \eta, y_{01}). \quad (13)$$

The input point in the upper right corner is set as the fourth input point, and the coordinates of the corresponding output point can be represented as:

$$(x_{04}, y_{04}) = (x_{03}, y_{03}). \quad (14)$$

By analyzing the coordinate transformation formula, it is possible to obtain the coordinates of the four vertices of the rotated digital image, as shown below:

$$\begin{cases} (x_{01}, y_{01}) = (O \times \cos \alpha_1 + x_0, O \times \sin \alpha_1 + y_0) \\ (x_{02}, y_{02}) = (-O \times \sin \alpha_2 + x_0, O \times \cos \alpha_2 + y_0) \\ (x_{03}, y_{03}) = (O \times \sin \alpha_2 + x_0, -O \times \cos \alpha_2 + y_0) \\ (x_{04}, y_{04}) = (-O \times \cos \alpha_1 + x_0, -O \times \sin \alpha_2 + y_0) \end{cases}. \quad (15)$$

Represent the rotation center point of Table A; B represents the horizontal C shift of the coordinate point; Represents the rotation of coordinate points.

Using the above method, the coordinates of the input point and corresponding output point are preliminarily corrected for geometric distortion in the digital image. However, in order to obtain a clearer image, normalization and rotation judgment of the image are also required. The process is as follows:

- (1) Automatic threshold segmentation is performed on the image, while contour segmentation is performed on the digital image.
- (2) Using morphology to cut the contour of installation holes in the image, the first black pixel point is detected and obtained in the image. If it is a black pixel point in the connected area, it is set as the starting point of recursion, and then continuous expansion is carried out until all pixels in the connected area are obtained.
- (3) Normalize the segmentation results for all images.
- (4) Determine whether the image needs to be rotated, and ultimately achieve geometric distortion correction of digital images.

4.2 Image Denoising Processing

In the measurement process of the engine end cover, high-precision electrical control and mechanical devices need to be coordinated. Therefore, in the actual visual inspection source image acquisition process, the equipment in the production workshop and the visual system itself will introduce external or internal noise to the image, such as electromagnetic waves, mechanical vibration noise, communication noise, etc. Therefore, noise reduction processing is a necessary means to improve measurement accuracy [14], This article uses median filtering method to process images.

The median filtering algorithm [15] is a non-linear filtering and smoothing algorithm that sets the grayscale value of each pixel as the median of all grayscale values of pixels within a certain neighborhood window of that point. When filtering noise points, the median algorithm first finds the grayscale median point $W_2[f(m, n)]$ of the filtering window in the image signal containing noise points, with each point (m, n) as the center; Then, calculate the weighting coefficients for each point within the window based on the median value $Median(W_2[f(m, n)])$; Finally, the grayscale values of each pixel in the window are summed up with the corresponding pixel weights, and the result is output as the new grayscale value $f_2(m, n)$ for point (m, n) . The expression of the median algorithm is:

$$g = med(x_1, x_2, \dots, x_n) = \begin{cases} \omega_k(m, n) \cdot x^{\frac{n+1}{2}} \\ \frac{1}{2} \omega_k(m, n) \cdot \left[x^{\frac{n}{2}} + x^{\frac{n+1}{2}} \right] \end{cases} \quad (16)$$

In the formula, n is the number of pixels in the filtering window, and $\omega_k(m, n)$ is the weight corresponding to each pixel in the filtering window $W_2[f(m, n)]$. The identification method is:

$$\omega_k(m, n) = \frac{1 / \left(1 + \left(f_k(m, n) - Median(W_2[f(m, n)]) \right)^2 \right)}{\sum_{k=1}^n 1 / \left(1 + \left(f_k(m, n) - Median(W_2[f(m, n)]) \right)^2 \right)} \quad (17)$$

The conventional median filtering algorithm is prone to interference from salt and pepper noise during weighted summation. Therefore, in order to improve the image preprocessing effect of this article, the median filtering is improved [16].

1) Select a filtering window W centered on each point in the engine end cover image, then remove the maximum and minimum pixel points within the window, and solve for the median $Median(P[f(m, n)])$ of the pixels in the remaining pixel set P .

2) Normalize each pixel group in set P , and set the absolute difference between the grayscale values of each pixel in set P and the median $Median(P[f(m, n)])$ to Δk , then:

$$\Delta k = |P_k - Median(P[f(m, n)])| \quad (18)$$

The average value of Δk is T :

$$T = \frac{\sum_{k=1}^n |P_k - \text{Median}(P[f(m,n)])|}{N}. \quad (19)$$

If the absolute difference between the grayscale value of a point within P and its mean value Δk is greater than the threshold T , then the weight is determined by Δk ; If Δk is less than the threshold T , the weight is determined by T .

3) Weighting all pixels in set P with their corresponding weights, and using the result as the output of the filtering window D center point. The expression of the improved median algorithm is:

$$f_2(m,n) = \sum_{k=1}^N (P_k(i,j) \cdot \omega_k(m,n)). \quad (20)$$

4.3 Extracting the Contour of Circular Hole Features

The engine end cover image and its detection circular hole are the ROI of the algorithm. In order to improve the efficiency of image processing, a threshold segmentation image preprocessing method is needed to extract ROI. In this paper, a conventional threshold segmentation algorithm is used to process the image. After threshold segmentation, the Canny edge detection algorithm is used to extract the contour of the circular hole [17]. The process is as follows:

- 1) After filtering the image, the smoothed image is obtained, and the image pixels are represented as $C(x, y)$;
- 2) Calculate gradient amplitude and direction: Use the Sobel operator to calculate the grayscale gradient in the horizontal and vertical directions of the image. The expression for gradient amplitude and direction is:

$$\begin{cases} S(x, y) = \sqrt{p_x^2 + p_y^2} \\ D(x, y) = \arctan\left(\frac{p_x}{p_y}\right) \end{cases} \quad (21)$$

In the formula, $S(x, y)$ represents the pixel gradient amplitude, $D(x, y)$ represents the pixel gradient direction, p_x represents the pixel gradient in the x direction, and p_y represents the pixel gradient in the y direction [18].

- 3) Perform non maximum suppression on the gradient amplitude to obtain all contour edge points;
- 4) Use the lag threshold method to filter out the true edge contours, and set the minimum and maximum thresholds for setting the gradient amplitude. If they are between the two, then there are true edge points in the neighborhood of the point, that is, true edge points. After processing, the detected edge contours are shown in Fig. 3.

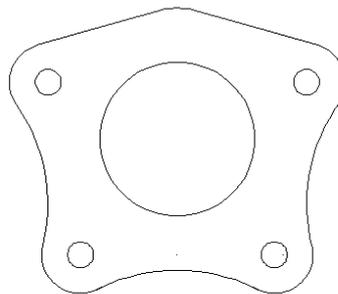


Fig. 3. Feature contour

5 Implementation of Image Feature Measurement Algorithm

The least squares curve fitting [19] and Hough transform curve fitting [20] are two widely used fitting methods. In order to reduce the error between visual measurement data and actual dimensions, this article uses the Hough transform curve fitting algorithm to process observation data, which can avoid the generation of redundant curves and also improve data processing speed. The fitting process is as follows:

1) Use the contour screening method based on the surrounding area to separate the circular hole contour of the workpiece, and obtain the separated inner and outer contours as shown in Fig. 4.

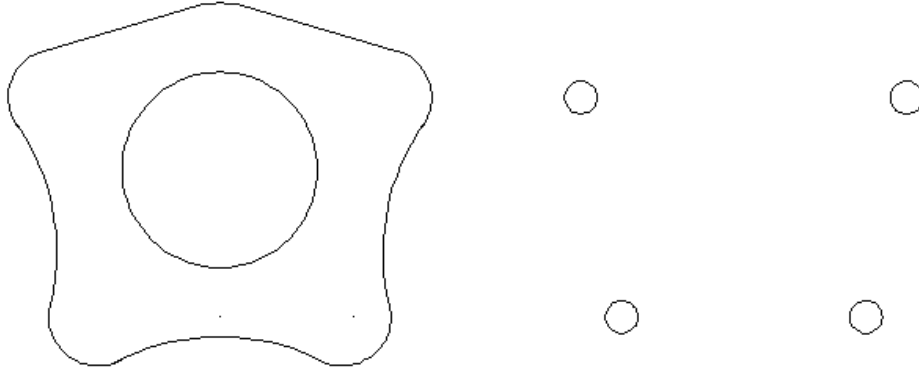


Fig. 4. Separating contours

2) Find the center of the circular hole, calculate the distance from each edge point on the circular hole to the center, and take the average value l from the edge point to the center. The coordinate formula of the center point is expressed as:

$$\begin{cases} C_x = \frac{\sum_{i=1}^N x_i}{N} \\ C_y = \frac{\sum_{i=1}^N y_i}{N} \end{cases} \quad (22)$$

(C_x, C_y) is the center pixel coordinate, N is the number of contour edge points, and (x_i, y_i) is the pixel coordinate of the i -th edge point in the outer contour edge point set.

3) Using the Hough transform fitting method to fit the points on a circular hole, denote the point set as $M(x_i, y_i)$, and the expression is:

$$(x - x_c)^2 + (y - y_c)^2 = r^2. \quad (23)$$

$$\sum_{i=1}^n [M(x, y) - M(x_i, y_i)]^2 = \min. \quad (24)$$

According to the Hough transform fitting, the property of minimizing the sum of squared distances is required:

$$\begin{bmatrix} \sum_{i=1}^N x_i^2 & \sum_{i=1}^N x_i y_i \\ \sum_{i=1}^N x_i y_i & \sum_{i=1}^N y_i^2 \end{bmatrix} \rightarrow \min. \tag{25}$$

According to the mapping relationship, a point on a circle in the image coordinate system corresponds to a conical surface of a spatial solid in the parameter coordinate system. Take any three points (x_1, y_1) , (x_2, y_2) , and (x_3, y_3) on the engine end cover. These spatial cones are mapped from points in the image coordinate system through a certain transformation relationship. All cones have a common intersection point, which is (x_c, y_c, s) , and the first two terms are their corresponding coordinates in the image coordinate system [21]. The schematic diagram of the fitting process of the engine end cover is shown in Fig. 5.

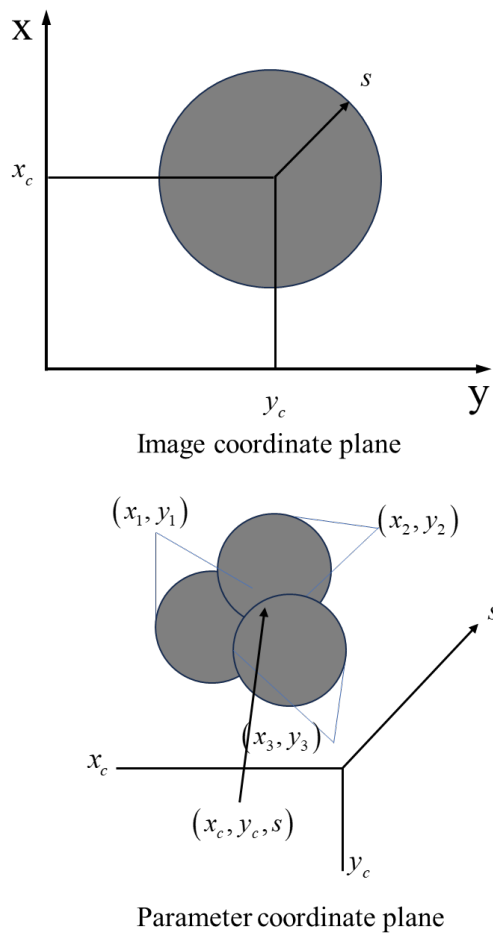


Fig. 5. Schematic diagram of curve fitting principle

Therefore, all circles are assumed to be the objects of interest to be fitted, and then only the circle with the largest radius is retained through code implementation for fitting to obtain the outer contour dimensions of the wheel hub, and finally obtain the measurement results.

The fitting process of the contour curve of the engine end cover is as follows:

- a. Reset the accumulation system to facilitate the mapping of the following two coordinate systems;

- b. Filter the points in the image coordinate system and timely convert the obtained points to the parameter coordinate system;
- c. The accumulator saves and accumulates the converted data;
- d. Using the peak point of data fluctuation as the condition for judging the curve.

6 Measurement System Design

After the construction of the visual system and a clear selection process, the system can preprocess the collected images, and then extract and measure the detection features. Therefore, based on the application scenario and necessary functional attributes, this section mainly introduces the design scheme and method of the visual inspection system, and completes the construction of the system framework and the design of the system main interface. Finally, the diameter of the circular hole on the engine end cover was measured using this system, and the measurement results were provided.

6.1 Detection System Design

This article is based on the Visual Studio 2019 development tool installed in the Windows 11 system environment, using C++ language combined with OpenCV open-source visual image processing library to design visual detection algorithms, using the WinForm framework in C# language to design human-machine interaction interfaces, and using MySQL database to manage and apply system data [22]. The overall system scheme is shown in Fig. 6.

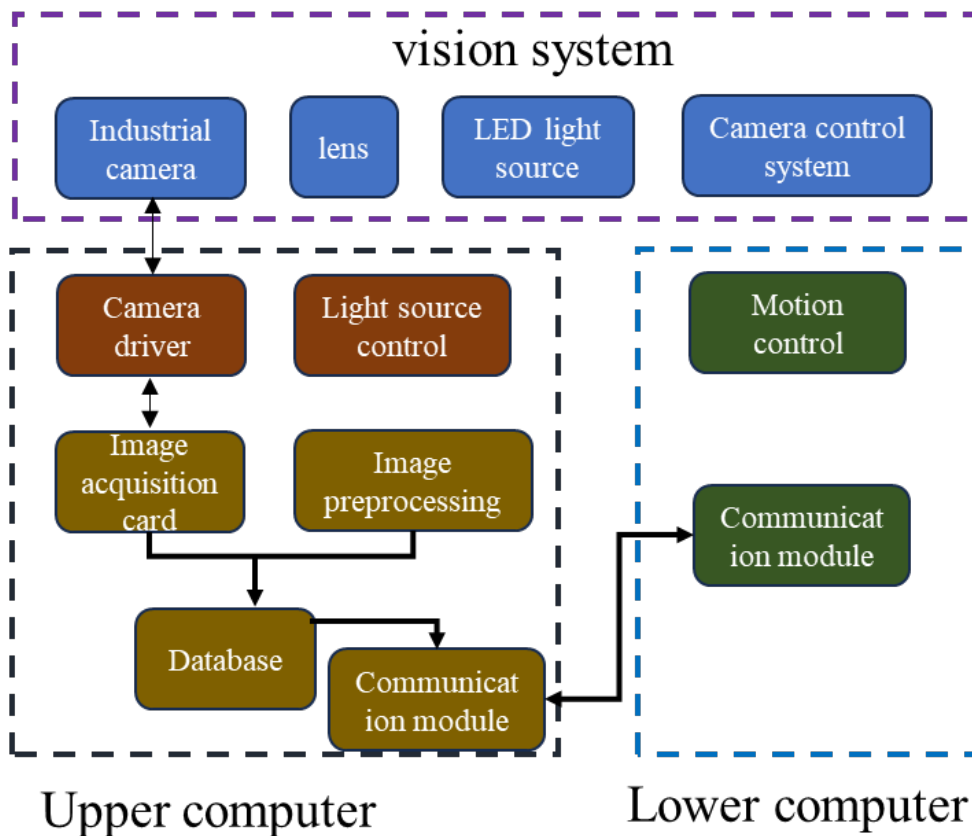


Fig. 6. Visual inspection software framework structure

The GUI interface design of the detection system is shown in Fig. 7.

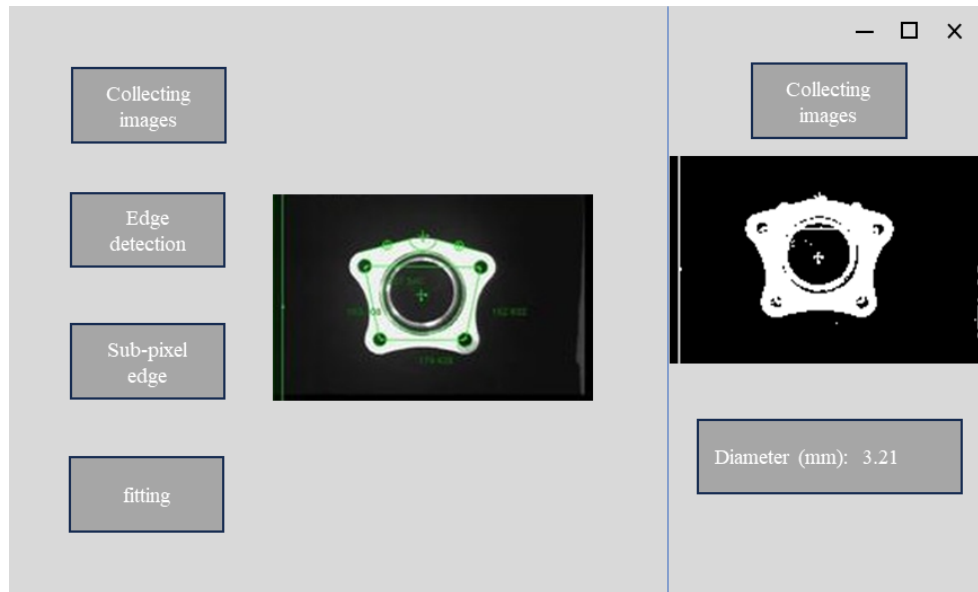


Fig. 7. The GUI interface design of the detection system

6.2 Analysis of Testing Experiment Results

Collect 12 photos of standard workpieces from different positions and angles, measure the diameter of circular holes using the method proposed in this article, and compare it with traditional measurement methods. The comparison results are shown in Table 2.

Table 2. Comparison of measurement results

Frequency	Actual measurement results	System measurement results	Systematic error	Average error
1	3.21	3.214	0.004	0.014
2	3.21	3.213	0.003	
3	3.21	3.214	0.004	
4	3.21	3.199	-0.011	
5	3.21	3.211	0.001	
6	3.21	3.211	0.001	
7	3.21	3.216	0.006	
8	3.21	3.199	-0.011	
9	3.21	3.203	-0.007	
10	3.21	3.208	-0.002	
11	3.21	3.211	0.001	
12	3.21	3.207	-0.003	

According to the analysis in the table above, the maximum error of the inner diameter measurement results of the improved algorithm is 0.011mm, the minimum error is 0.001mm, and the average error is 0.014mm; The experimental results show that the measurement error of this system can be controlled within 0.015mm, and the average error is effectively reduced. The system has good stability and can meet the accuracy requirements of industrial testing.

7 Conclusion

This article uses machine vision technology to measure small-sized workpieces, and finally takes the measurement of engine end cover installation holes as an example to verify the feasibility of the proposed method. Firstly, based on actual work needs, in terms of component selection, resolution, image size, light source, and other factors were fully considered, and the visual system was built; Then, for the image data collected by the image acquisition card, in order to improve the accuracy of visual detection, the visual graphics are preprocessed, including image correction, image denoising, and image feature extraction; Finally, the design and implementation of an online measurement scheme for image features were carried out, and the development of an image measurement system was completed. In the experiment of measuring the circular hole on the engine end cover, the measurement accuracy met production requirements.

After further research and reflection, it was found that this article can be further improved in the following areas:

1) The scenario described in this article is the production of large quantities of small workpieces, and the production speed is constantly improving. Therefore, the requirements for detection speed in long-term production scenarios are also constantly increasing. Although the research content of this article is online detection, the detection speed cannot match the actual production speed.

2) When extracting edge features of detection objects, this article uses Hough transform fitting and makes corresponding improvements. However, this method is more suitable for fitting curve contours. In actual production, there will be linear features, and the extraction and measurement of linear features should be supplemented to make the measurement method and system provided in this article more adaptable to measurement.

References

- [1] H.-L. Zhang, H.-W. Li, G.-D. Yu, F. Miao, J.-M. Wang, L. Ji, Research on Detection Method of Riveting Aperture Size Based on Algorithm of Caliper Edge Detection, *Tool Engineering* 56(12)(2022) 141-146.
- [2] X.-D. Yu, G. Yin, C.-D. Zhu, X.-C. Xie, An Efficient Measuring Method for Hole Size of Parts Based on Image Processing Technology, *Computer Measurement & Control* 30(9)(2022) 60-66.
- [3] B.-X. Yan, M.-L. Dong, M. Zong, Design of Step-Style Work Piece Measurement Method Based on Computer-Vision, *Machinery Design & Manufacture* (4)(2017) 140-143.
- [4] H.-J. Bao, S.-Y. Liu, Z. Ren, Y.-H. Zhang, Z.-Y. Hu, Y.-P. Ge, Sprocket size measurement method based on machine vision, *Journal of Jilin University (Engineering and Technology Edition)* 53(10)(2023) 2795-2806.
- [5] C. Bi, K.-S. Pi, B. Sheng, K. Long, X. Hao, Measurement Technology of Blade-shaped Holes Based on Machine Vision, *Tool Engineering* 56(12)(2022) 147-151.
- [6] X.-A. Chen, H. Deng, J.-H. Zhou, X.-C. Yu, Dynamic Measurement Method of Rail Round Hole Based on Machine Vision, *Electronic Measurement Technology* 45(21)(2022) 111-116.
- [7] Z.-C. Shu, S.-X. Cao, Q. Jiang, Z.-P. Xu, X.-D. Lou, Positioning and Dimension Measurement of Micro-channel Heat Exchangers Based on 3D Vision, *Acta Metrologica Sinica* 43(9)(2022) 1128-1134.
- [8] S.-J. Zhang, X.-T. Mo, Y.-L. Dong, Y. Cheng, X.-S. Huang, Spherical catadioptric imaging visual measurement system for internal thread pitch, *Journal of Electronic Measurement and Instrumentation* 37(10)(2023) 221-220.
- [9] S.-K. Li, C. Qiao, R.-J. Hong, M. Hu, Measuring Method of Gear End Face Height Based on Binocular Stereo Vision, *Tool Engineering* 57(10)(2023) 135-138.
- [10] J. Kong, Q. Li, L.-M. Wang, H.-T. Liu, B.-J. Wang, H.-H. Cui, Optimal Calibration Method of Dual-Vision Measurement Experimental System for Assembly Docking, *Aeronautical Manufacturing Technology* 66(12)(2023) 14-20.
- [11] L.-F. Du, Z. Zhou, T.-Q. Wang, Dimension measurement of aluminum alloy hub based on machine vision, *Journal of Machine Design* 39(S2)(2022) 193-198.
- [12] H. Zhao, Q.-M. Chen, C.-G. Li, W.-X. Yang, Research on Robot Automatic Wiring Method Integrating Machine Vision and Tactile Sense, *Computing Technology and Automation* 41(4)(2022) 84-90.
- [13] C.-Y. Dang, L.-G. Jia, Z.-Q. Zeng, W.-H. Du, A method for measuring round holes of bimetallic castings based on machine vision, *Manufacturing Technology & Machine Tool* (6)(2021) 96-99.
- [14] Y. Wang, Q.-F. Li, J.-Y. Qi, Image Denoising Method Based on Improved Adaptive Median Filter, *Ship Electronic Engineering* 42(6)(2022) 112-115.
- [15] F.-Q. Zhao, Image Denoising Algorithm Based on Improved Median Filter, *Computer & Digital Engineering* 51(2)(2023) 292-295+444.
- [16] L. Mei, S.-Q. Xun, Application of weighted median filtering algorithm in denoise of magnetic resonance imaging, *Journal of Yanbian University (Natural Science Edition)* 47(4)(2021) 365-369.

- [17] Y.-C. Guo, M.-J. Li, M.-G. Liu, T.-Y. Ao, Improved Algorithm for Edge Detection of Building Cracks Based on Canny Operator, *Computer Simulation* 39(11)(2022) 360-365+410.
- [18] C.-J. Sun, X.-Y. Duan, H. Wang, Z.-C. Chen, P. Xu, Research of Parts Pose Estimation Method Based on Boundary Feature Matching, *Machine Design & Research* 39(3)(2023) 109-114.
- [19] Y.-J. Liu, P. Han, J.-X. Ma, Greedy orthogonal least squares identification algorithm based on Householder transformation, *Control and Decision* 37(9)(2022) 2281-2286.
- [20] W.-L. Li, Z.-F. Liang, Q. Fang, A Multi Threshold Hough Transform Lane Detection Algorithm, *Journal of Xiamen University of Technology* 29(5)(2021) 1-7.
- [21] X.-K. Wang, B. Liu S.-Y. Jiang, Z.-X. Yu, G.-G. Ban, B. Li, Research on the Measurement Method of Conductor Diameter Based on Binocular Vision, *Modern Manufacturing Technology and Equipment* 58(12)(2022) 86-89.
- [22] F. Li, Z.-F. Wang, Y.-L. Liu, Y.-S. Lu, Design of intelligent inspection and control system for flexible circuit board based on machine vision, *Electronic Test* 36(22)(2022) 40-42.